NPQH derivatives were essentially identical with those previously reported for the DMGH analogues.[2]

Corresponding procedures for the BQDH analogues were similar except that the reactions were generally run at 25 °C or lower owing to the faster rates (see Table III). For $Fe(BQDH)_2(MeIm)(PBu_3)$ a variation in procedure was required owing to the trans effect $PBu_3 > MeIm$ in this system. For the determination k^N_{-P} an excess of MeIm (300 μL) was added to 3 mL of a stock solution of $Fe(BQDH)_2(PBu_3)_2$. The initial fast reaction to give $Fe(BQDH)_2(MeIm)(PBu_3)$ was complete in seconds, and the subsequent slower reaction was monitored with time. For the determination of k^P_{-N} at −23 °C, solid $Fe(BQDH)_2(MeIm)_2$ was dissolved in a toluene solution containing 10^{-4} M PBu_3 and 7.5×10^{-4} M MeIM and the mixture was left to stand until a spectrum containing primarily $Fe(BQDH)_2(MeIm)(PBu_3)$ with ~20% $Fe(BQDH)_2(PBu_3)_2$ and negligible $Fe(BQDH)_2(MeIm)_2$ was obtained. Excess PBu_3 was then added to obtain k^P_{-N} independent of $[PBu_3]$ from 0.025 to 0.1 M.

Kinetics. Reactions in which CO was the entering ligand were carried out under 1 atm of CO. Otherwise, all reactions were routinely run in serum-capped nitrogen-purged cuvettes and monitored by visible spectroscopy. Temperatures were maintained by means of water circulation through a thermostatable cell holder. Temperatures were read directly from an RTD device attached to the cell holder.

Reaction solutions were prepared by injecting either the ligand (either by itself or as a toluene solution) into a dilute solution of the complex or the more concentrated solution of the complex into a thermostated toluene solution of the ligand.

In all cases rates were found to be invariant to a 10-fold variation of the entering ligand (typically 0.03–0.3 M). Reactions for species generated in situ were always carried out with the entering ligand in at least 50-fold excess over the leaving ligand. Complex concentrations for kinetic runs were typically 10^{-4} M or less.

Rate constants for reactions involving a single pseudo-first-order rate were obtained from a least-squares fit of $\log [(A - A_\infty)/(A_0 - A_\infty)]$ vs. time using a microcomputer analysis as described elsewhere.[2] For reactions involving two consecutive first-order rates of comparable magnitude, absorbance data vs. time at several wavelengths were analyzed by computer comparison of observed and calculated absorbance as described previously.[2] Photolyses were carried out with white light or 100 Å band-pass interference filters.

Acknowledgment. Support of the National Sciences and Engineering Research Council of Canada is gratefully acknowledged.

Contribution from the Department of Chemistry,
University of Victoria, Victoria, British Columbia, Canada V8W 2Y2

^{31}P and ^{195}Pt NMR Studies and the Crystal and Molecular Structure of Chloro(triethylphosphine)[tris(diphenylphosphinothioyl)methyl]platinum(II), $[PtCl(PEt_3)\{C(PPh_2S)_3\}]$, an S,S-Bonded Chelate with Dynamic Stereochemistry Controlled by One Labile and One Inert Pt–S Bond

Jane Browning, Kathryn Anne Beveridge, Gordon William Bushnell, and Keith Roger Dixon*

Received September 25, 1985

Reaction of $CH(PPh_2S)_3$ with $[Pt_2Cl_4(PEt_3)_2]$ or $[Pt_2Cl_2(PEt_3)_4][BF_4]_2$ results in spontaneous deprotonation of the ligand to form $[PtCl(PEt_3)\{C(PPh_2S)_3\}]$ (I) or $[Pt(PEt_3)_2\{C(PPh_2S)_3\}][BF_4]$ (II), respectively. Compound I crystallizes as a dichloromethane solvate in the monoclinic space group $P2_1/c$, with a = 16.902 (3) Å, b = 13.999 (2) Å, c = 19.771 (3) Å, and β = 93.03 (2)°, and the structure was refined to R = 0.0561 (R_w = 0.0725) by using 3635 independently measured reflections. The square-planar platinum coordination involves only two of the sulfur atoms (Pt–S = 2.282 (3) and 2.351 (4) Å), and the methanide carbon is closely planar with P–C–P angles from 116.2 (7) to 124.2 (7)°. In solution at temperatures above ca. 50 °C, I undergoes a dynamic intramolecular process in which the noncoordinated sulfur exchanges with the coordinated sulfur trans to triethylphosphine. The Pt–S bond trans to chloride remains inert and serves as a pivot for the exchange process. The differing Pt–S bond strengths implied by this process are reflected in both the bond lengths, 2.282 (3) Å trans to Cl and 2.351 (4) Å trans to P, and in the two-bond Pt–P NMR coupling constants, 128 and 48 Hz, respectively. Compound II undergoes a related exchange process except that both Pt—S bonds are labilized by trans phosphine ligands and all three P═S groups of the ligand are involved in the exchange. ^1H, $^{13}C\{^1H\}$, $^{31}P\{^1H\}$, and $^{195}Pt\{^1H\}$ NMR spectra are reported for both complexes, and the exchange processes are studied in detail by ^{31}P NMR to yield $\Delta G^{\circ\ddagger}$ values of 67.1 and 61.3 kJ mol^{-1} for I and II, respectively.

Introduction

The ligands $CH(PPh_2)_3$, $CH(PPh_2S)_3$, and $[C(PPh_2S)_3]^-$ have attracted recent attention.[1-4] For example, the ability of a polydentate ligand to maintain the integrity of a cluster unit during a catalytic reaction is of obvious interest, and complexes in which $CH(PPh_2)_3$ coordinates to a triangular cluster face have been reported.[1] Although this is also possible in principle for the sulfur derivatives, it appears that their coordination chemistry is rather different. Thus in reactions with Hg(II) or Cd(II) salts, coordination of $CH(PPh_2S)_3$ is accompanied by deprotonation to form complexes in which $[C(PPh_2S)_3]^-$ functions as a uninegative, tridentate ligand toward a single metal center.[2,3] Related complexes of Cu(I), Ag(I), and Au(I) can be prepared by reactions of metal salts with $[n\text{-}Bu_4N][C(PPh_2S)_3]$.[4] This behavior is similar to that found for the well-known tripyrazolylborates, which appear to be the only previous examples of this rather rare class of ligands.[5,6] However, whereas some complexes of the tripyrazolylborates exhibit a bidentate, fluxional coordination mode, for example in $[Pd(\eta\text{-}C_3H_5)(HB(pz)_3)]$,[5,6] only the tridentate mode has been reported to date for $[C(PPh_2S)_3]^-$.

We have recently reported a novel coordination mode for a closely related ligand, $[CH(PPh_2S)_2]^-$. In the complex $[PtCl(PEt_3)\{CH(PPh_2S)_2\}]$ this ligand is a C,S-bonded chelate, but in solution at ambient temperature the coordinated and noncoordinated P═S groups undergo continuous dynamic interchange.[7] It was therefore of considerable interest to investigate the platinum complexes of $CH(PPh_2S)_3$ and $[C(PPh_2S)_3]^-$ to determine whether these exhibit any coordination modes other than the tridentate coordination found in the metal complexes described above. The present paper describes the results of this study. The complexes are S,S-bonded chelates that exhibit dynamic, intramolecular interchange of coordinated and noncoordinated P═S groups. The nature of the interchange and the site at which it occurs are

(1) Bahsoun, A. A.; Osborn, J. A.; Voelker, C.; Bonnet, J. J.; Lavigne, G. *Organometallics* **1982**, *1*, 1114.
(2) Grim, S. O.; Smith, P. H.; Satek, L. C. *Polyhedron* **1982**, *1*, 137.
(3) Grim, S. O.; Nittolo, S.; Ammon, H. L.; Smith, P. H.; Colquhoun, I. J.; McFarlane, W.; Holden, J. R. *Inorg. Chim. Acta* **1983**, *77*, L241.
(4) Grim, S. O.; Sangokoya, S. A.; Gilardi, R. D.; Colquhoun, I. J.; McFarlane, W. Presented at the 23rd International Conference on Coordination Chemistry; Boulder, CO, 1984.
(5) Trofimenko, S. *Acc. Chem. Res.* **1971**, *4*, 17.
(6) Trofimenko, S. *Chem. Rev.* **1972**, *72*, 497.
(7) Browning, J.; Bushnell, G. W.; Dixon, K. R.; Pidcock, A. *Inorg. Chem.* **1983**, *22*, 2226.

0020-1669/86/1325-1987$01.50/0

critically dependent on the nature of the ligands trans to the coordinated sulfur(s).

Experimental Section

(a) Synthesis and Spectroscopic Studies. Data relating to the characterization of the complexes are given in the tables, in the Results section, and in the preparative descriptions below. Microanalyses were performed by the Canadian Microanalytical Service, Vancouver, BC, Canada. Melting points were recorded in open capillary tubes and are uncorrected.

^1H, ^{31}P, ^{13}C, and ^{195}Pt NMR spectra were recorded at 250.1, 101.3, 62.9, and 53.5 MHz, respectively, by using a Bruker WM250 Fourier transform spectrometer locked to the solvent deuterium resonance. The solvent was $CDCl_3$ except for the variable-temperature runs in $(CD_3)_2SO$ as noted in the text. For ^{31}P, ^{13}C, and ^{195}Pt spectra, protons were decoupled by broad-band ("noise") irradiation at appropriate frequencies. ^1H and ^{13}C chemical shifts were measured relative to external $Si(CH_3)_4$. ^{31}P chemical shifts were measured relative to external $P(OMe)_3$ and are reported in ppm relative to 85% H_3PO_4, with a conversion factor of +141 ppm. ^{195}Pt chemical shifts are reported in ppm relative to $\Xi(^{195}Pt) = 21.4$ MHz.[8] For all nuclei, positive chemical shifts are downfield of the appropriate reference shift. Simulated NMR spectra were calculated on an IBM 3083 computer and plotted on a Tektronix 4013 graphics screen for preliminary work or a Calcomp 1039 plotter for final data. The programs used were a locally constructed package based on DNMR3[9] for dynamic spectra and line shape analysis, and UEAITR[10] and NMRPLOT[11] for static spectra and iterative refinement and plotting.

Except as noted below, all operations were carried out under an atmosphere of dry nitrogen by using standard Schlenk tube techniques. Solvents were dried by appropriate methods and distilled under nitrogen prior to use. $CH(PPh_2S)_3$,[12] $[Pt_2Cl_4(PEt_3)_2]$,[13] and $[Pt_2Cl_2(PEt_3)_4][BF_4]_2$[14] were prepared as previously described.

$[PtCl(PEt_3)\{C(PPh_2S)_3\}]$. A solution of $CH(PPh_2S)_3$ (0.17 g, 0.26 mmol) in acetone (10 mL) was added dropwise to a stirred solution of $[Pt_2Cl_4(PEt_3)_2]$ (0.10 g, 0.13 mmol) in acetone (15 mL). Sodium perchlorate monohydrate (0.037 g, 0.26 mmol; in a small volume of acetone) was then added and the mixture stirred for 2 h, during which time a slight cloudiness developed. The solvent was removed in vacuo, the residue extracted with dichloromethane, and the solvent again removed in vacuo. The residue was extracted with acetone and diethyl ether added dropwise to the extract to give $[PtCl(PEt_3)\{C(PPh_2S)_3\}]$ (0.25 g, 0.25 mmol) as yellow crystals, mp 175–177 °C. Anal. Calcd for $C_{43}H_{45}ClP_4PtS_3$: C, 51.0; H, 4.48. Found: C, 51.1; H, 4.74.

$[Pt(PEt_3)_2\{C(PPh_2S)_3\}][BF_4]$. A solution of $CH(PPh_2S)_3$ (0.24 g, 0.36 mmol) in dichloromethane (15 mL) was added dropwise to a stirred solution of $[Pt_2Cl_2(PEt_3)_4][BF_4]_2$ (0.20 g, 0.18 mmol) in dichloromethane (15 mL). Stirring was continued for a few minutes before removal of the solvent in vacuo. The residue was dissolved in acetone and filtered through Celite and charcoal. Dropwise addition of diethyl ether to the filtrate gave $[Pt(PEt_3)_2\{C(PPh_2S)_3\}][BF_4]$ (0.38 g, 0.32 mmol) as colorless crystals, mp 254–256 °C dec. Anal. Calcd for $C_{49}H_{60}BF_4P_5PtS_3$: C, 49.8; H, 5.12. Found: C, 49.8; H, 5.08.

(b) X-ray Data Collection. Crystals of $[PtCl(PEt_3)\{C(PPh_2S)_3\}]$ were grown by vapor diffusion of diethyl ether into a solution of the complex in dichloromethane. Photographic work (Weissenberg and precession cameras, Cu Kα radiation) gave the symmetry and an approximate unit cell before the crystals were transferred to a Picker four-circle diffractometer automated with a PDP11/10 computer and using Zr-filtered Mo Kα radiation ($\lambda = 0.71069$ Å). The unit cell was refined by least-squares methods with 34 pairs of centering measurements at $\pm 2\theta$ in the range $|2\theta| = 14$–$36°$. The crystal was mounted approximately along the c axis. Crystal data at ~26 °C: monoclinic, space group $P2_1/c$; $a = 16.902$ (3), $b = 13.999$ (2), $c = 19.771$ (3) Å; $\beta = 93.03$ (2)°; V(cell) = 4671 (1) Å^3; $D_m = 1.53$ g cm^{-3} (flotation in CCl_4/m-xylene), $D_c = 1.56$ g cm^{-3}; formula $C_{44}H_{47}Cl_3P_4PtS_3$; $M_r = 1097.38$; $Z = 4$; asymmetric unit, one molecule of complex plus one molecule of CH_2Cl_2. Intensity measurements were collected for two reciprocal space octants (h unrestricted, $k \geq 0$, $l \geq 0$) up to $2\theta = 40°$. A $\theta/2\theta$-step scan was used with 100 steps of 0.01° in 2θ, counting for 0.40 s/step. Background measurements were for 20 s at each end of the scan. Each batch of 50 reflections was preceded by the measurement of three standard reflections (006, 020, and 400). The Lorentz and polarization factors were applied, and each batch was scaled to maintain the sum of the standards constant. There was no evidence of sample decomposition. Absorption corrections were applied with a numerical integration procedure utilizing a Gaussian grid (4 × 4 × 8). The crystal shape was defined by perpendicular distances to crystal faces from a central origin as follows: ±{100}, 0.0328 mm; ±{010}, 0.090 mm; ±{001}, 0.222 mm. The absorption coefficient was 36.26 cm^{-1} (transmission factors 0.52–0.79). The low-angle reflection 100 and reflections with intensity less than $2.0\sigma(I)$ were removed from the data set to give a final file containing 3635 independent reflections.

(c) Structure Solution and Refinement. The structure was solved by using SHELX-76,[15] and illustrations were drawn with ORTEP.[16] Atomic scattering factors were for neutral atoms, corrected for anomalous dispersion.[17] The structure was solved by direct methods, completed by standard Fourier synthesis procedures using difference maps, and refined by least-squares techniques minimizing $\Sigma w\Delta^2$ where $\Delta = ||F_o| - |F_c||$. Weights were from counting statistics using $w = 1/(\sigma^2(F) + 0.001F^2)$. Hydrogen atoms were not included, carbon atoms were treated isotropically, and the heavier atoms were treated anisotropically, giving 276 variable parameters. The maximum shift/esd ratio was 0.62 for a parameter of the main molecule, but convergence for the CH_2Cl_2 molecule was more difficult (maximum shift/esd ratio was 1.55). Residuals were $R = 0.0561$ and $R_w = (\Sigma w\Delta^2/\Sigma wF_o^2)^{1/2} = 0.0725$. The final difference map (max +1.46 e Å^{-3}; min −0.81 e Å^{-3}) gave no indication that any material had been overlooked.

Results

(A) Synthesis. The complexes $[PtCl(PEt_3)\{C(PPh_2S)_3\}]$ (I) and $[Pt(PEt_3)_2\{C(PPh_2S)_3\}][BF_4]$ (II) are readily prepared by bridge-cleavage reactions of appropriate chloro-bridged platinum dimers with $CH(PPh_2S)_3$. The dimers were $[Pt_2Cl_4(PEt_3)_2]$ for I and $[Pt_2Cl_2(PEt_2)_4][BF_4]_2$ for II.

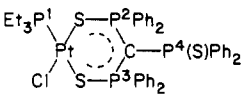

I

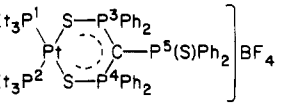

II

The reaction to form I proceeds more cleanly and gives a higher yield if sodium perchlorate is added to the reaction mixture (in acetone) in order to remove chloride as insoluble sodium chloride. In preparations of both I and II, loss of the methine proton to form the anionic ligand occurred readily in acetone and a more basic solvent was not needed. Some reactions were carried out in which the anion was generated from $CH(PPh_2S)_3$ with butyl lithium before reaction with the platinum complex, but although the products were essentially the same, they were less pure and yields were lower.

The complexes were characterized mainly by the crystal structure and $^{31}P\{^1H\}$ NMR spectroscopy described below. However, ^1H, $^{13}C\{^1H\}$, and $^{195}Pt\{^1H\}$ NMR spectra were also fully consistent with the assigned structures and served to confirm some of the structural detail. Thus ^1H spectra of both I and II showed aromatic (δ 6.8–8.3), methylene (δ 1.65 and 1.91, respectively), and methyl (δ 0.87 and 0.91) resonances with the expected integrated intensity ratios. The chief features of interest are the absence of detectable absorption in the methine proton region (δ ~6)[18] for either complex, which confirms the deprotonation of the ligands, and the typical cis phosphine pattern[19] in the methyl region of II. $^{13}C\{^1H\}$ spectra yielded essentially the same information. For I the methyl and methylene regions were at δ 7.52 and 13.66, respectively, and gave $^1J(P\text{–}C) = 36.5$, $^2J(P\text{–}C) = 2.0$,

(8) Kidd, R. G.; Goodfellow, R. J. In *NMR and the Periodic Table*; Harris, R. K., Mann, B. E., Eds.; Academic: London, 1978; p 249.
(9) Kleier, D. A.; Binsch, G. *Quantum Chemistry Program Exchange, Program No. 165*; University of Indiana: Bloomington, IN, 1969.
(10) Johannsen, R. B.; Ferreti, J. A.; Harris, R. K. *J. Magn. Reson.* **1970**, *3*, 84.
(11) Swalen, J. D. In *Computer Programs for Chemistry*; Detar, D. F., Ed.; W. A. Benjamin: New York, 1968; Vol. 1.
(12) Issleib, K.; Abicht, H. P. *J. Prakt. Chem.* **1970**, *312*, 456.
(13) Goodfellow, R. J.; Venanzi, L. M. *J. Chem. Soc.* **1965**, 7533.
(14) Dixon, K. R.; Hawke, D. J. *Can. J. Chem.* **1971**, *49*, 3252.
(15) Sheldrick, G. M. *SHELX-76. A Computer Program for Crystal Structure Determination*; University of Cambridge: Cambridge, England, 1976.
(16) Johnson, C. K. *ORTEP*; Report ORNL-3794, Oak Ridge National Laboratory: Oak Ridge, TN, 1965.
(17) Cromer, D. T.; Waber, J. T. *International Tables for X-ray Crystallography*; Ibers, J. A., Hamilton, W. C., Eds.; Kynoch: Birmingham, England, 1974; Vol. IV, pp 99, 148.
(18) Grim, S. O.; Sangokoya, S. A.; Colquhoun, I. J.; McFarlane, W. *J. Chem. Soc., Chem. Commun.* **1982**, 930.
(19) Dixon, K. R.; Moss, K. C.; Smith, M. A. R. *Can. J. Chem.* **1974**, *52*, 692.

Table I. Rate Constants k_r (s^{-1}) for Phosphorus Interchange in I ([PtCl(PEt$_3$){C(PPh$_2$S)$_3$}]) and II ([Pt(PEt$_3$)$_2${C(PPh$_2$S)$_3$}][BF$_4$])

temp, K	303	313	323	333	343	353	363	373	383	393	403	418
I		<30	70	115	225	375	550	1100	1800	3000	4500	7500
II	150	300	400	800	1200	2000	3000	4500	...	...	...	$<10^4$

^2J(Pt–C) = 35.3, and ^3J(Pt–C) ~ 20 Hz. The aromatic region (δ 125–135) contained at least 15 resonances, showing that rotation of the phenyl rings is restricted by steric constraints as it is in the parent ligand, CH(PPh$_2$S)$_3$.[20] No resonance was detected for the unique, central carbon of the anionic ligand (δ 33.1 in the free anion[18]). This is not unexpected in view of the lack of attached hydrogen and the expected high multiplicity. The $^{13}C\{^1H\}$ spectrum of II was basically similar except that resolution was poor in the aromatic region (undoubtedly a consequence of the dynamic processes described below) and that the methylene carbon resonance was the X region of an AA'X pattern corresponding to a J(AA') (i.e. ^2J(P–Pt–P)) value of about 20 Hz. The small magnitude of this coupling confirms the mutually cis arrangement of the two PEt$_3$ ligands on the platinum center.[21,22] Other data were as follows: δ(aromatic) 125–135, δ(methylene) 15.73, δ(methyl) 8.15; ^1J(P–C) = 36.7 Hz; ^2J(P–C) < 2.0 Hz, ^2J(Pt–C) ~ 20 Hz, ^3J(Pt–C) = 22.0 Hz.

The $^{195}Pt\{^1H\}$ spectrum of I consisted of a doublet of doublets of doublets centered at Ξ 21.408021 MHz (δ +374.80). The major coupling of 3275 Hz is clearly ^1J(Pt–P), and the other doublets show couplings of 128 and 48 Hz. Normal trans-influence criteria[23] would indicate that the larger of these two couplings is due to ^2J(Pt–P) trans to Cl and the smaller to ^2J(Pt–P) trans to PEt$_3$. ^4J(Pt–P) is not resolved. The ^{195}Pt spectrum of II showed only a triplet (Ξ 21.395095 MHz, δ –229.19) due to ^1J(Pt–P). Each component of the triplet showed additional poorly resolved fine structure due to the [C(PPh$_2$S)$_3$]$^-$ ligand.

(B) Phosphorus-31 NMR and Dynamic Stereochemistry. (i) Compound I. The $^{31}P\{^1H\}$ NMR spectrum of I, recorded in CDCl$_3$ solution at ~30 °C, is shown in Figure 1A. It is readily interpreted in terms of the static structure I. The peak at +8.49 ppm, which shows pseudotriplet structure, is unambiguously assigned to P(1) since it shows sidebands due to coupling with ^{195}Pt (33.8% abundant) and the large magnitude of this coupling must indicate a one-bond connection (^1J(Pt–P) = 3277 Hz). The triplet structure results from two approximately equal doublet couplings, ^3J(1,2) = 7.7 and ^3J(1,3) = 7.2 Hz, with ^5J(1,4) not resolved. The most shielded resonance, δ +42.29, shows no evidence of platinum sidebands and must therefore be due to P(4). It consists of an overlapping doublet of doublets, ^2J(2,4) = 13.5 and ^{2}J(3,4) = 16.6 Hz. The remaining resonances at +25.32 and +35.29 ppm both consist of the expected doublets of doublets of doublets, ^2J(2,3) = 27.9 Hz and are readily assigned to P(2) and P(3), respectively, by the magnitudes of the Pt–P couplings. The upfield sideband of the P(2) resonance is obscured by overlapping with the P(1) sideband but the downfield sideband is clearly visible and gives ^2J(Pt–P(2)) as approximately 125 Hz, in agreement with the ^{195}Pt spectrum discussed above. The smaller value of ^{2}J(Pt–P(3)) trans to phosphorus makes the sidebands more difficult to observe on the P(3) resonance, but expanded-scale spectra made it clear that the peak contour near the base is consistent with the coupling of 48 Hz observed in the ^{195}Pt spectrum.

When the temperature is rasied, the P(3) and P(4) resonances of compound I begin to broaden while peaks due to P(1) and, more surprisingly, P(2), remain sharp. At 60 °C, the highest temperature accessible in CDCl$_3$ solution, this process had only just begun and higher temperature studies were conducted in (CD$_3$)$_2$SO solution. There was some evidence that the donor properties of (CD$_3$)$_2$SO may accelerate the process relative to the process in CDCl$_3$ solution, but the effect was small and it was impossible to be certain because of the slow rates over the temperature range accessible in CDCl$_3$. Selected spectra showing the complete process in (CD$_3$)$_2$SO with final averaging of the P(3) and P(4) resonances to a single peak are shown as Figure 1B–D, and data relating to a complete selection of temperatures are collected in Table I. Note that the ambient-temperature spectrum, Figure 1A, was recorded in CDCl$_3$ because this gave the best resolution, but spectra in (CD$_3$)$_2$SO were essentially identical except for slight differences in the chemical shifts and in ^1J(Pt–P). The P(1) and P(2) regions remained unchanged over the temperature range studied except for slight temperature dependence of the shifts and ^1J(Pt–P).

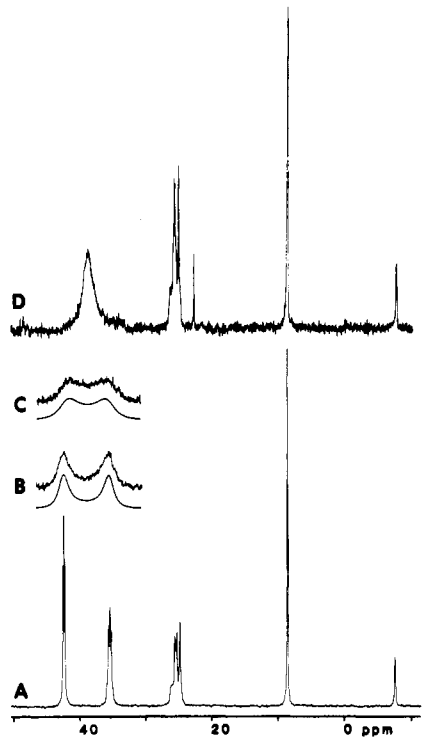

Figure 1. $^{31}P\{^1H\}$ nuclear magnetic resonance spectra of I ([PtCl(PEt$_3$){C(PPh$_2$S)$_3$}]) at 101.3 MHz: (A) 303 K in CDCl$_3$; (B) 363 K in (CD$_3$)$_2$SO with computer simulation; (C) 373 K in (CD$_3$)$_2$SO with computer simulation; (D) 403 K in (CD$_3$)$_2$SO.

The spectra shown in Figure 1 clearly demonstrate that compound I, in solution at elevated temperatures, undergoes a dynamic process in which the S=P(4) group exchanges with S=P(3). When we allow for minor temperature shifts, the single signal observed for these two phosphorus atoms at the fast-exchange limit is at the average of the chemical shifts of the coordinated and noncoordinated groups in the slow-exchange spectrum. This observation rules out a high-temperature situation where S=P(3) and S=P(4) are both noncoordinated and the fourth site on Pt is occupied by solvent. The rate constants (k_r) for the exchange process over a range of temperatures have been derived from computer line-shape fitting with the DNMR3 program of Kleier and Binsch,[9] and the results are shown in Figure 1 and Table I. From this data, an Eyring plot of ln (k_r/T) against $1/T$ gave a good straight line, and comparison with the standard transition state theory equation[24]

$$\ln (k_r/T) = -\Delta H^{\circ\ddagger}/RT + \Delta S^{\circ\ddagger}/R + \ln (k/h)$$

(20) Colquhoun, I. J.; McFarlane, W.; Bassett, J. M.; Grim, S. O. *J. Chem. Soc., Dalton Trans.* **1981**, 1645.
(21) Nixon, J. F.; Pidcock, A. *Annu. Rev. NMR Spectrosc.* **1969**, *2*, 345.
(22) Pregosin, P. S.; Kunz, R. W. *^{31}P and ^{13}C NMR of Transition Metal Phosphine Complexes*; Springer-Verlag: New York, 1979.
(23) Appleton, T. G.; Clark, H. C.; Manzer, L. E. *Coord. Chem. Rev.* **1973**, *10*, 335.
(24) Amdur, I.; Hammes, G. G. *Chemical Kinetics*; McGraw-Hill: New York, 1966; pp 55, 56.

Table II. Rate Plots and Thermodynamic Parameters for Phosphorus Interchange in I ($[PtCl(PEt_3)\{C(PPh_2S)_3\}]$) and II ($[Pt(PEt_3)_2\{C(PPh_2S)_3\}][BF_4]$)

		I	II
ln k_r vs. $1/T$	slope	−6832 ± 120	−5469 ± 136
	intercept	25.31 ± 0.33	23.07 ± 0.41
	correlation	0.9988	0.9981
ln (k_r/T) vs. $1/T$	slope	−6466 ± 119	−5133 ± 136
	intercept	18.40 ± 0.33	16.25 ± 0.40
	correlation	0.9986	0.9979
E_a, kJ mol^{-1}		56.8	45.5
$\Delta H^{\circ\ddagger}$, kJ mol^{-1}		53.8	42.7
$\Delta S^{\circ\ddagger}$, J K^{-1}		−44.6	−62.4
$\Delta G^{\circ\ddagger}$, kJ mol^{-1}		67.1	61.3

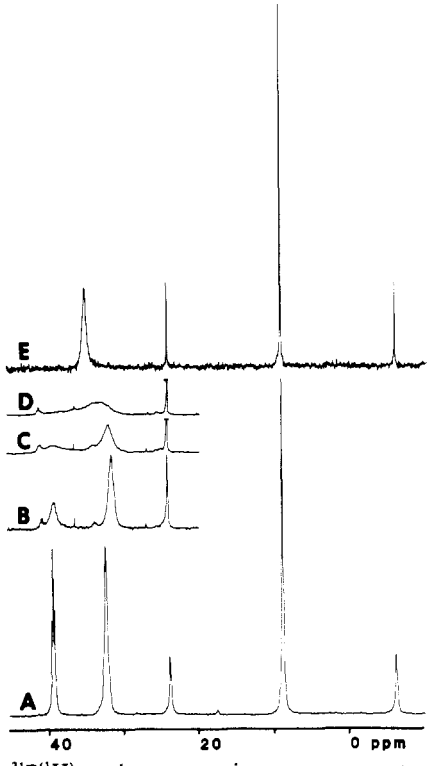

Figure 2. $^{31}P\{^1H\}$ nuclear magnetic resonance spectra of II ($[Pt(PEt_3)_2\{C(PPh_2S)_3\}][BF_4]$) at 101.3 MHz: (A) 223 K in $CDCl_3$; (B) 303 K in $(CD_3)_2SO$; (C) 323 K in $(CD_3)_2SO$; (D) 343 K in $(CD_3)_2SO$; (E) 418 K in $(CD_3)_2SO$.

enabled $\Delta H^{\circ\ddagger}$, $\Delta S^{\circ\ddagger}$, and hence $\Delta G^{\circ\ddagger}$, to be calculated (Table II). This table also includes an Arrhenius activation energy, E_a, which was derived from the slope of an Arrhenius plot (ln k_r against $1/T$) assuming

$$\ln k_r = -E_a/RT + \ln A$$

(ii) Compound II. $^{31}P\{^1H\}$ spectra of II recorded at ambient temperature showed that a dynamic process, similar to that described above for I, was already relatively fast at this temperature. Accordingly the spectrum was recorded at −50 °C in $CDCl_3$, and this spectrum is shown in Figure 2A. The resonance at +8.82 ppm has platinum sidebands (^1J(Pt–P) = 3056 Hz) and is clearly due to triethylphosphine, P(1,2), in structure II. By analogy with compound I, the remaining resonances at +32.40 and +39.50 ppm may be assigned to P(3,4) and P(5) respectively, and this is confirmed by the 2:1 integrated intensity ratio of the two peaks and also by the broadening at the base of the P(3,4) resonance, indicating the presence of overlapping ^{195}Pt sidebands. The triplet structure of the P(5) resonance is satisfactorily explained by coupling to P(3,4) (^2J(P–P) = 16.0 Hz), but the origin of the band shapes for P(3,4) and P(1,2) is not immediately obvious. Since our characterization of the compound depends primarily on this spectral analysis, it is important to clarify the point. In principle, the P(1,2) and P(3,4) resonances should each be half of an AA′XX′ spin system, with the P(3,4) region doubled by the further

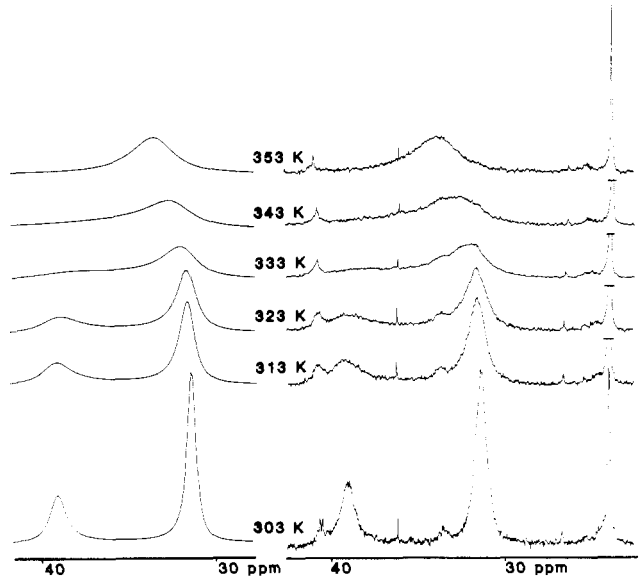

Figure 3. $^{31}P\{^1H\}$ nuclear magnetic resonance spectra of II ($[Pt(PEt_3)_2\{C(PPh_2S)_3\}][BF_4]$) at 101.3 MHz in $(CD_3)_2SO$. The right-hand set is observed spectra, and corresponding computer simulations are shown on the left.

coupling to P(5). Since the P(1,2) resonance appears as a poorly resolved doublet with a separation of about 5 Hz and the P(3,4) resonance can be regarded as two such doublets separated by about 16 Hz (i.e. J(3,5)), the problem is to determine conditions under which half of an AA′XX′ spin system takes this poorly resolved doublet form. The well-known literature values for *cis*-P–Pt–P couplings[21,22] and the comparison with compound I enable J(1,2) and J(3,4) to be estimated as 20 and 30 Hz, respectively, and in this spin system the signs of these two couplings are unimportant.[25] Using these two values, computer simulations showed that a fit with the observed spectrum can then be obtained provided that J(1,3) and J(1,4) are of opposite sign and differ in magnitude by about 5 Hz. For example respective values of 12 and −7 Hz give a good fit. However, only J(3,5), 16.0 Hz, can be properly determined from the spectrum.

Preliminary variable-temperature NMR spectra of compound II indicated no significant rate differences for the dynamic process in $CDCl_3$ or $(CD_3)_2SO$ solution up to +60 °C, and a complete line shape study was then carried out in the latter solvent. The results were analyzed as described above for compound I and are presented in Figures 2 and 3 and Tables I and II. The dynamic process differs from that observed in compound I in that all three P=S groups are now involved in the exchange, the P(3,4) and P(5) resonances collapsing to a single peak at +145 °C, as would be expected since both Pt–S bonds are now labilized by a trans triethylphosphine ligand.

(C) Structure of $[PtCl(PEt_3)\{C(PPh_2S)_3\}]$. The atomic labeling scheme and the structure of a single molecule of compound I are shown in Figure 4. Fractional atomic coordinates and isotropic temperature parameters and selected bond lengths and angles are collected in Tables III and IV, and further tables of anisotropic temperature factors, structure factors, complete bond lengths and bond angles, and selected intermolecular distances have been deposited as supplementary material.

The structure of I shows a simple, mononuclear platinum coordination compound with only two of the three P=S groups involved in the coordination. The six-membered PtS_2P_2C ring is in boat form with the most striking deviation from the cyclohexane type of structure being the S(1)–Pt–S(2) angle of 94.9(1)°. The square plane about platinum is considerably distorted, with the metal in Figure 1 lying about 0.1 Å below the plane of the ligating atoms. The boat conformation of the six-membered ring

(25) Pople, J. A.; Schneider, W. G.; Bernstein, H. J. *High-Resolution Nuclear Magnetic Resonance*; McGraw-Hill: New York, 1959; p 142.

Table III. Fractional Atomic Coordinates and Temperature Parameters[a]

atom	x/a	y/b	z/c	U_{iso}, Å^2
Pt	82482 (3)	54263 (4)	40673 (3)	412 (2)′
Cl(1)	9122 (3)	4832 (3)	3294 (2)	80 (2)′
Cl(2)	9006 (8)	2531 (9)	2021 (6)	272 (8)′
Cl(3)	8319 (9)	3782 (10)	1089 (7)	301 (9)′
S(1)	7470 (2)	6022 (2)	4877 (2)	41 (1)′
S(2)	8761 (2)	6920 (3)	3768 (2)	56 (1)′
S(3)	6878 (3)	10218 (3)	4436 (2)	56 (1)′
P(1)	6708 (2)	7032 (2)	4485 (2)	37 (1)′
P(2)	8242 (2)	7976 (3)	4289 (2)	45 (1)′
P(3)	6716 (2)	9078 (2)	3866 (2)	37 (1)′
P(4)	7942 (2)	3917 (3)	4352 (2)	53 (1)′
C(1)	6984 (10)	3783 (12)	4784 (8)	76 (5)
C(2)	6766 (11)	2731 (14)	4956 (10)	102 (6)
C(3)	8764 (11)	3394 (13)	4898 (10)	88 (6)
C(4)	9016 (12)	4052 (14)	5512 (10)	99 (6)
C(5)	7891 (10)	3006 (12)	3664 (9)	76 (5)
C(6)	7211 (12)	3292 (14)	3138 (11)	106 (7)
C(7)	7200 (7)	8008 (8)	4192 (6)	37 (3)
C(8)	9104 (23)	3691 (28)	1595 (21)	221 (15)
C(11)	6134 (7)	7253 (9)	5219 (7)	43 (3)
C(12)	6113 (8)	8159 (9)	5490 (7)	47 (4)
C(13)	5646 (10)	8329 (11)	6060 (8)	72 (5)
C(14)	5237 (10)	7608 (13)	6326 (9)	84 (5)
C(15)	5280 (9)	6671 (11)	6091 (8)	69 (5)
C(16)	5736 (8)	6507 (10)	5511 (7)	57 (4)
C(21)	6042 (7)	6472 (9)	3856 (7)	42 (3)
C(22)	5229 (9)	6392 (11)	3953 (8)	63 (4)
C(23)	4728 (11)	5929 (13)	3434 (9)	84 (5)
C(24)	5067 (11)	5593 (12)	2892 (10)	85 (5)
C(25)	5903 (11)	5652 (12)	2766 (9)	80 (5)
C(26)	6388 (8)	6123 (10)	3285 (7)	55 (4)
C(31)	8536 (8)	7929 (10)	5199 (7)	53 (4)
C(32)	8166 (9)	8532 (11)	5630 (8)	65 (4)
C(33)	8373 (11)	8495 (13)	6340 (10)	89 (6)
C(34)	8928 (10)	7806 (12)	6571 (9)	77 (5)
C(35)	9283 (9)	7258 (11)	6171 (8)	71 (5)
C(36)	9102 (10)	7295 (11)	5432 (8)	72 (5)
C(41)	8702 (8)	9048 (10)	3947 (7)	49 (4)
C(42)	8854 (8)	9049 (10)	3259 (7)	54 (4)
C(43)	9213 (10)	9843 (12)	2976 (9)	74 (5)
C(44)	9439 (11)	10591 (13)	3398 (10)	86 (6)
C(45)	9304 (12)	10595 (13)	4092 (10)	94 (6)
C(46)	8933 (10)	9775 (11)	4374 (8)	68 (5)
C(51)	5645 (7)	8847 (9)	3736 (6)	38 (3)
C(52)	5108 (8)	9133 (9)	4215 (7)	49 (4)
C(53)	4316 (9)	8994 (11)	4111 (8)	62 (4)
C(54)	4009 (9)	8570 (11)	3529 (8)	63 (4)
C(55)	4521 (8)	8252 (10)	3035 (7)	54 (4)
C(56)	5350 (8)	8387 (9)	3136 (7)	50 (4)
C(61)	7013 (7)	9304 (8)	3008 (6)	35 (3)
C(62)	7114 (8)	8555 (9)	2561 (7)	48 (4)
C(63)	7305 (8)	8780 (10)	1887 (7)	55 (4)
C(64)	7417 (9)	9690 (11)	1694 (8)	69 (5)
C(65)	7338 (9)	10445 (11)	2138 (8)	64 (4)
C(66)	7116 (8)	10255 (9)	2808 (7)	48 (4)

[a] Estimated standard deviations are given in parentheses. Coordinates $\times 10^n$ where $n = 5$ for Pt and $n = 4$ otherwise. Temperature parameters $\times 10^n$ where $n = 4$ for Pt and $n = 3$ otherwise. Primed values indicate that U_{eq} is given. U_{eq} = the equivalent isotropic temperature parameter. $U_{eq} = {}^1/_3 \sum_i \sum_j U_{ij} a_i^* a_j^* (a_i a_j)$. $T = \exp -(8\pi^2 U_{iso}(\sin^2\theta)/\lambda^2)$.

determines the disposition of the phenyl groups, and the distortion of the coordination plane is probably caused by the various steric interactions between these groups and the chloride and triethylphosphine ligands. The Pt–Cl, 2.331 (4) Å, and Pt–P, 2.254 (4) Å, bond lengths are both in the middle of the normal ranges for these bonds, 2.27–2.45 and 2.23–2.32 Å, respectively,[26,27] as is expected for bonds trans to a ligating atom of intermediate trans influence such as sulfur. The Pt–S bonds, 2.282 (3) and 2.351

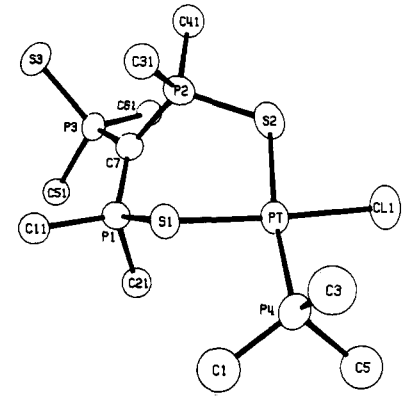

Figure 4. ORTEP plot of I ([PtCl(PEt$_3$){C(PPh$_2$S)$_3$}]). In the interests of a clear representation of the coordination geometry, the figure shows only the first atoms of the three ethyl groups (C(1,2), C(3,4), and C(5,6)) attached to P(4) and the three pairs of phenyl groups ((C11–16) and C(21–26), (C31–36) and C(41–46), and (C51–56) and C(61–66)) attached to P(1), P(2), and P(3), respectively. The structure also contained a molecule of methylene chloride (C(8), Cl(2,3)). A complete ORTEP plot is provided as Figure 4S in the supplementary material.

Table IV. Selected Interatomic Distances (Å) and Bond Angles (deg)[a]

Cl(1)–Pt	2.334 (4)	C(7)–P(2)	1.762 (12)
S(1)–Pt	2.282 (3)	C(31)–P(2)	1.841 (14)
S(2)–Pt	2.351 (4)	C(41)–P(2)	1.835 (14)
P(4)–Pt	2.254 (4)	C(7)–P(3)	1.809 (12)
P(1)–S(1)	2.038 (5)	C(51)–P(3)	1.844 (12)
P(2)–S(2)	2.027 (5)	C(61)–P(3)	1.821 (13)
P(3)–S(3)	1.964 (5)	C(1)–P(4)	1.880 (16)
C(7)–P(1)	1.717 (12)	C(3)–P(4)	1.864 (18)
C(11)–P(1)	1.815 (13)	C(5)–P(4)	1.862 (17)
C(21)–P(1)	1.811 (13)		
S(1)–Pt–Cl(1)	175.9 (1)	C(41)–P(2)–C(7)	112.3 (6)
S(2)–Pt–Cl(1)	84.1 (1)	C(41)–P(2)–C(31)	107.0 (6)
S(2)–Pt–S(1)	94.9 (1)	C(7)–P(3)–S(3)	115.0 (4)
P(4)–Pt–Cl(1)	89.5 (1)	C(51)–P(3)–S(3)	109.2 (4)
P(4)–Pt–S(1)	91.1 (1)	C(51)–P(3)–C(7)	109.0 (6)
P(4)–Pt–S(2)	171.6 (1)	C(61)–P(3)–S(3)	110.9 (4)
P(1)–S(1)–Pt	111.3 (2)	C(61)–P(3)–C(7)	109.5 (6)
P(2)–S(2)–Pt	110.3 (2)	C(61)–P(3)–C(51)	102.6 (6)
C(7)–P(1)–S(1)	111.9 (4)	C(1)–P(4)–Pt	114.9 (5)
C(11)–P(1)–S(1)	99.7 (4)	C(3)–P(4)–Pt	109.8 (6)
C(11)–P(1)–C(7)	115.0 (6)	C(3)–P(4)–C(1)	109.3 (8)
C(21)–P(1)–S(1)	108.6 (4)	C(5)–P(4)–Pt	117.5 (5)
C(21)–P(1)–C(7)	114.0 (6)	C(5)–P(4)–C(1)	104.8 (7)
C(21)–P(1)–C(11)	106.5 (6)	C(5)–P(4)–C(3)	99.2 (8)
C(7)–P(2)–S(2)	114.8 (4)	P(2)–C(7)–P(1)	116.2 (7)
C(31)–P(2)–S(2)	111.6 (5)	P(3)–C(7)–P(1)	124.2 (7)
C(31)–P(2)–C(7)	108.9 (6)	P(3)–C(7)–P(2)	119.4 (7)
C(41)–P(2)–S(2)	101.9 (5)		

[a] Estimated standard deviations are given in parentheses.

(4) Å, reflect the greatly differing trans influences of the chloride and tertiary phosphine ligands with the shorter Pt–S bond trans to the phosphine. All of these metal–ligand lengths are closely comparable with those observed previously for [Pt$_2$Cl$_2$(μ-SEt$_2$)(PEt$_3$)$_2$]: Pt–Cl, 2.34 Å; Pt–P, 2.26 Å; Pt–S trans to Cl, 2.27 Å; Pt–S trans to P, 2.37 Å.[28] This structure involves bridging sulfur atoms but the terminal Pt–S bonds in *cis*-[PtCl$_2$\{S-(C$_6$H$_4$Cl)$_2$\}$_2$] are similar in length, 2.285 Å.[29]

Within the phosphorus sulfide ligand the most important structural observation is the closely planar arrangement of phosphorus atoms around C(7). The P–C–P angles range from 116.2 (7) to 124.2 (7)°, and this trigonal arrangement about the carbon is clear confirmation of the deprotonation of the ligand

(26) Hartley, F. R. *Chem. Soc. Rev.* **1973**, *2*, 163.
(27) Mather, G. G.; Pidcock, A.; Rapsey, G. J. N. *J. Chem. Soc., Dalton Trans.* **1973**, 2095.
(28) Hall, M. C.; Jarvis, J. A. J.; Kilbourn, B. T.; Owston, P. G. *J. Chem. Soc., Dalton Trans.* **1972**, 1544.
(29) Spofford, W. A.; Amma, E. L.; Senoff, C. V. *Inorg. Chem.* **1971**, *10*, 2309.

during the formation of the complex.

Discussion

The dynamic process in $[PtCl(PEt_3)\{C(PPh_2S)_3\}]$ (I) is closely related to that which we have described previously for $[PtCl(PEt_3)\{CH(PPh_2S)_2\}]$ (III).[7] In the latter molecule the phosphorus

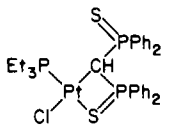

III

sulfide ligand is bound via a strong Pt–C bond, which provides a fixed pivot for the exchange of the coordinated and noncoordinated sulfur atoms of the ligand. This exchange is rapid on the NMR time scale at 25 °C, but the isomer of III in which the coordinated sulfur is trans to chlorine rather than trans to phosphorus is static at this temperature. The difference between these two isomers must reflect a labilization of the P=S group in III by the trans effect of the triethylphosphine ligand.[7] This phenomenon is even more dramatically illustrated by the present example since very similar Pt–S bonds must serve both for the fixed pivot and for the labile point of exchange. The difference between the two roles is produced merely by the different trans effects of the chloride and triethylphosphine ligands, which occupy the coordination positions trans to P(2) and P(3), respectively, in structure I. Even at 145 °C the Pt–S bond trans to chloride remains inert; P(2) does not participate in the exchange process, and its NMR signal remains sharp. With respect to this type of phenomenon it is usual to differentiate between the kinetic "trans effect", which may be caused by either ground-state or transition-state phenomena, and the "trans influence", which is a ground-state bond weakening as measured by parameters such as bond lengths or NMR coupling constants.[23,26] In the present case a difference in Pt–S bond strength is shown both in the bond lengths, 2.282 (3) Å trans to Cl and 2.351 (4) Å trans to P, and in the two-bond Pt–P coupling constants, 128 and 48 Hz, respectively. It is therefore probable that a ground-state bond weakening is responsible for the kinetic effect. Moreover, the dynamic behavior of $[Pt(PEt_3)_2\{C(PPh_2S)_3\}][BF_4]$ (II) confirms that the bond weakening is indeed a result of the trans influence since the introduction of the second triethylphosphine involves both coordinated P=S groups in the exchange process and also lowers the activation energy. Examples where the kinetic trans effect, NMR coupling constants, and bond lengths can be correlated in such a simple and direct way within a single molecule are very rare.

Acknowledgment. We thank the Natural Sciences and Engineering Research Council of Canada and the University of Victoria for research grants and C. Greenwood for recording NMR spectra.

Registry No. I, 101859-87-4; II, 101915-81-5; $[PtCl_4(PEt_3)_2]$, 15692-96-3; $[Pt_2Cl_2(PEt_3)_4][BF_4]_2$, 19394-82-2.

Supplementary Material Available: Complete ORTEP plot (Figure 4S), anisotropic temperature factors for the heavy atoms (Table S2), selected intermolecular distances (Table S3), complete bond lengths (Table S4), and complete bond angles (Table S5) (5 pages). Ordering information is given on any current masthead page. According to policy instituted Jan 1, 1986, the tables of calculated and observed structure factors (16 pages) are being retained in the editorial office for a period of 1 year following the appearance of this work in print. Inquiries for copies of these materials should be directed to the Editor.

Contribution from the Chemical Technology Division, Oak Ridge National Laboratory, Oak Ridge, Tennessee 37831

Raman Spectroscopic Studies of UO_2^{2+} Association with Hydrolytic Species of Group IV (4)† Metals

S. A. Sherrow,* L. M. Toth, and G. M. Begun‡

Received October 14, 1985

Raman spectra have been obtained of UO_2^{2+} in hydrolyzed Zr(IV) and Hf(IV) solutions and of UO_2^{2+} adsorbed by solid hydrous ZrO_2, HfO_2, and ThO_2. The symmetric stretching vibration (ν_1) of UO_2^{2+} was shifted from 872 to 835 cm^{-1} in the hydrolyzed metal solutions, indicating that UO_2^{2+} was complexed by the Zr(IV) and Hf(IV) hydrolytic species. Heating or aging of the solutions caused a substantial reduction in the amount of complexed UO_2^{2+}. The ν_1 band was observed at ~820 cm^{-1} in all of the hydrous oxide spectra. Although the spectra of the solid hydrous oxides indicated that UO_2^{2+} was similarly bound to all three, the behavior of UO_2^{2+} in hydrolyzed Zr(IV) and Hf(IV) solutions was significantly different from that reported for previous studies of UO_2^{2+} in hydrolyzed Th(IV) solutions. The observed differences are discussed and are related to the structures of the hydrolytic species. The changes in color and spectra reported for UO_2^{2+} in heated hydrolyzed Th(IV) solutions may be due to the formation of a distinct thorium(IV) uranate compound.

Introduction

Hydrolysis dominates the aqueous chemistry of the quadrivalent metals. Complexation, ion exchange, and solubility properties of the metals are profoundly affected by the presence of mono- and polynuclear hydrolysis products. The distribution of hydrolytic species is a complicated function of metal concentration, solution acidity, and concentration and identity of additional ions. In many cases, the chemistry is further complicated by the slow aggregation of hydrolysis products into polymeric hydroxides, which eventually precipitate from solution. A particularly troublesome example is the polymerization and precipitation of Pu(IV) in fuel reprocessing streams. While most published studies of hydrolysis[1] treat the behavior of a single metal ion in noncomplexing media, practical systems tend to be less ideal and often contain appreciable concentrations of several metal ions. In such systems, interactions between hydrolytic species may significantly alter the chemical behavior of the species of interest.

Previous investigations[2] in our laboratory showed that Pu(IV) polymerization and precipitation are inhibited by the presence of uranyl ion, UO_2^{2+}. Raman spectroscopic studies[3] revealed that

† The periodic group notation in parentheses is in accord with recent actions by IUPAC and ACS nomenclature committees. A and B notation is eliminated because of wide confusion. Groups IA and IIA become groups 1 and 2. The d-transition elements comprise groups 3 through 12, and the p-block elements comprise groups 13 through 18. (Note that the former Roman number designation is preserved in the last digit of the new numbering: e.g., III → 3 and 13.)

‡ Chemistry Division, Oak Ridge National Laboratory, Oak Ridge, TN 37831.

(1) A compilation and critical review of data through 1974 are given in: Baes, C. F.; Mesmer, R. E. *The Hydrolysis of Cations*; Wiley: New York, 1976: (a) pp 156–159; (b) pp 176–182; (c) pp 158–168.

(2) Toth, L. M.; Friedman, H. A.; Osborne, M. M. *J. Inorg. Nucl. Chem.* **1981**, *43*, 2929.

0020-1669/86/1325-1992$01.50/0